Received: 3 December 2020 | Revised: 18 January 2021 | Accepted: 22 February 2021

DOI: 10.1002/pip.3413

RESEARCH ARTICLE

PROGRESS IN PHOTOVOLTAICS WILEY

Influence of Ga back grading on voltage loss in low-temperature co-evaporated Cu(In,Ga)Se2 thin film solar cells

Shih-Chi Yang | Mario Ochoa | Ramis Hertwig | Abdessalem Aribia | Ayodhya N. Tiwari | Romain Carron

Laboratory for Thin Films and Photovoltaics, Empa - Swiss Federal Laboratories for Materials Science and Technology, Dübendorf, Switzerland

Correspondence
Shih-Chi Yang, Laboratory for Thin Films and Photovoltaics, Empa - Swiss Federal Laboratories for Materials Science and Technology, Überlandstrasse 129, 8600 Dübendorf, Switzerland.
Email: shih-chi.yang@empa.ch

Funding information
Bundesamt für Energie, Grant/Award Number: SI/501614-01; Horizon 2020 Framework Programme, Grant/Award Number: EMPIR project HyMet; Swiss State Secretary for Education, Research and Innovation (SERI), Grant/Award Number: 17.00105 (EMPIR project HyMet)

Abstract

The performance of Cu(In,Ga)Se_2 (CIGS) solar cells is limited by the presence of the highly recombinative CIGS/Mo interface. The recombination at the CIGS/Mo interface is influential for the open circuit voltage (V_{OC}) in high quality CIGS absorbers with increased charge carriers diffusion length. A quantitative understanding of the role of the Ga back grading height (ΔGGI) in suppressing back interface recombination is needed. In this work, we take advantage of a low temperature process to modify the ΔGGI while keeping the composition in the notch and front regions almost unchanged. Improvement in both V_{OC} deficit and time-resolved photoluminescence lifetime are observed with increasing ΔGGI. With a combination of back surface modification experiments and numerical simulations, we quantify a voltage loss in ungraded devices of approximately 100 mV solely from the back interface recombination. Nice agreement between simulation and experimental data is reached while constraining the values of possible diffusion lengths. Our results suggest that a ΔGGI of about 0.50 is required to effectively suppress the back interface recombination, highlighting the importance of grading control in high-performance CIGS solar cells and devices.

KEYWORDS
back interface recombination, Ga back grading, TRPL lifetime, V_{OC} deficit

1 | INTRODUCTION

Thin film solar cells based on polycrystalline Cu(In,Ga)Se_2 (CIGS) have reached efficiencies of 23.35%[1] on glass and 20.8%[2] on flexible substrates thanks to years of intensive research and continuous investigations. High efficiency CIGS absorbers are commonly designed with varying [Ga]/([Ga] + [In]) (GGI) ratios throughout the thickness. The value of GGI affects the bandgap through the position of the conduction band minimum but has little effect on the valence band maximum.[3] In typical double-graded CIGS absorbers, the Ga concentration first decreases from the CdS/CIGS interface to a minimum inside the absorber, which is known as 'notch', and then increases towards the CIGS/Mo back interface.[4] The Ga back grading plays an important role in minimizing the recombination at the CIGS/Mo interface by reducing the electron density in its vicinity. To increase the efficiency of CIGS solar cells towards the theoretical limit, it is required to gain a comprehensive understanding of electrical loss mechanisms caused by different back grading profiles.

The copyright line for this article was changed on 15 April 2021 after original online publication

The concept of Ga back grading was first introduced by Contreras et al.[5] Since this breakthrough, Ga back grading was widely investigated by both simulations and experiments. Dullweber *et al*.[6] reported that the back grading suppresses back interface recombination and results in a significant enhancement in the open circuit voltage (V_{OC}). Following studies also showed the instrumental influence of notch position, the ratio of back and front grading heights[7,8] and explored different defect models and doping concentrations.[9] Moreover, addressing the back interface recombination is crucial with thin or ultra-thin CIGS absorbers.[10,11] Despite diverse research results, a wide range of back grading height (ΔGGI) values are reported for high efficiency solar cells,[1,2,12,13] generally ranging from 0.15 to 0.60. There is no conclusive agreement about minimum required ΔGGI. In addition, the quality of state-of-the-art absorbers considerably improved following breakthroughs and developments of the past 10 years, leading to longer diffusion length.[14] It makes the control of back interface recombination become even more critical. A quantitative assessment of the impact of ΔGGI on the electrical losses is therefore required. However, experimental investigations are not straightforward, because tuning the ΔGGI value generally also affects the elemental distributions in the notch and front regions, introducing other dependencies in the electrical loss difficult to disentangle.

In this work, we take advantage of a low-temperature CIGS deposition process (≈450°C) to modify the back grading. The less pronounced In-Ga inter-diffusion at low temperature allows an improved control and steeper slopes of the GGI grading.[15] It also allows for almost unchanged grading in the notch and front region. We compare the experimental V_{OC} deficit ($V_{OC,def} = E_g / q - V_{OC}$) and changes in V_{OC} calculated from time-resolved photoluminescence (TRPL) transients in absorbers with different back grading heights. We modify the back surfaces of CIGS absorbers to assess the influence of back surface recombination as a limiting factor for higher V_{OC}. Furthermore, numerical simulations of voltage loss for absorbers with different ΔGGI and diffusion lengths are also performed and further compared with experimental data. Our work provides direct guidelines to design graded absorbers with reducing voltage loss for high efficiency CIGS solar cells. The methodology developed in this study can help research groups and industries to improve the control on back grading height and further quantify and minimize the electrical loss arising from back interface recombination.

2 | EXPERIMENTAL AND SIMULATIONS

CIGS absorbers were grown by co-evaporation method with a multi-stage low-temperature deposition process (about 450°C) as described in Avancini et al.[16] on Mo-coated (approx. 500 nm thick by sputtering) soda-lime glass substrates. A SiO_x barrier layer below the Mo back contact was deposited by reactive sputtering to prevent uncontrolled diffusion of alkali elements from the substrates. The multi-stage co-evaporation process consists of: a first stage (≈350°C) in which Ga and In are evaporated; a second stage (≈450°C) in which Cu is evaporated while In and Ga evaporation rates are reduced by about one order of magnitude; a third stage (≈450°C) in which only Ga and In are deposited to reach an overall Cu-poor composition. Se overpressure is provided throughout all stages. During the third stage, In evaporation rate is kept constant while the Ga rate is slightly increased, leading to the desired front grading. At the end of the deposition, the In shutter is closed for 30 seconds after the Ga shutter. A series of samples with different ΔGGI was produced by modifying In and Ga rates in the first stage as discussed in details in Section 3. The absorbers were sequentially treated with sodium fluoride (NaF) and rubidium fluoride (RbF) post-deposition treatments (PDTs) of 20 minutes each in Se ambient at about 350°C. The integrated GGI and [Cu]/([Ga] + [In]) (CGI) values of CIGS absorbers were determined by X-ray fluorescence (XRF) measurements, previously calibrated with a reference.

The cells were completed with a 30 nm cadmium sulfide (CdS) buffer layer by chemical bath deposition, an RF-sputtered window layer consisting of a 80 nm intrinsic zinc oxide (ZnO) and a 200 nm Al-doped (Al_2O_3 2wt.%) ZnO, electron beam evaporated Ni/Al grids and a MgF_2 anti-reflective coating. Cells of approximately 0.57 cm^2 area were defined by mechanical scribing. A 30 nm Al_2O_3 passivation layer was deposited on the back side of selected CIGS absorbers by the atomic layer deposition (ALD) to modify the back interface recombination after Mo delamination. The process was performed at a substrate temperature of 200°C with argon as carrier gas at a pressure of 25 Pa in a Fiji G2 system (Veeco Instruments Inc.). The precursors were trimethylaluminium TMA and H_2O. The growth rate was determined by ellipsometry on Si (100) reference substrates and linear growth was observed with a rate of 0.99 Å $cycle^{-1}$.

Current–voltage (J–V) parameters were measured using a four-terminal Keithley 2400 source meter under standard test conditions (25°C, 1000 W/m^2 AM1.5G illumination, ABA-class sun simulator). External quantum efficiency (EQE) was measured using a chopped illumination from a halogen light source, wavelength-selected with a double-grating monochromator. A halogen lamp bias with about 0.2 sun intensity was applied during the measurements. A certified Si solar cell was used for calibration. Capacitance–voltage (C-V) profiles were measured with an Agilent E4980A LCR meter at a frequency of 1 kHz and a temperature of 300 K. Carrier concentrations were extracted from the apparent doping curve at an applied voltage of zero assuming an n^+p junction.

Compositional depth profiles were measured by time-of-flight secondary ion mass spectrometry (SIMS). The primary beam was 25 keV Bi^+ with total current of 0.6 pA and a raster size of 100 × 100 μm^2. The sputtering beam was 250 nA, 2 keV O^{2+} with an on-sample area of 300 × 300 μm^2. GGI depth profiles were determined by scaling the elemental traces with integral GGI values obtained from XRF. TRPL measurements were performed using a 639 nm diode laser with 100 ps pulse duration as excitation source, and an InGaAs photomultiplier in combination with a PicoQuant time correlated single photon counting electronics for signal acquisition. Pulse repetition rates were 0.3, 0.2 and 0.1 MHz for the absorbers before delamination, after delamination and after Al_2O_3 deposition. The illumination spot size was around 130 μm diameter. The corresponding photon density was around 7×10^{11} cm^{-2} per pulse. Before TRPL measurements, the

window layers were etched away in acetic acid, leaving a thin CdS layer on the absorber. Cross-section images were acquired using a Hitachi S-4800 scanning electron microscope (SEM).

Numerical simulations were carried out within the framework of Sentaurus drift-diffusion simulator from Synopsis.[17] A double graded absorber with a thickness of 2 μm has been considered and divided into three different regions, namely the front grading, notch and back grading. The front grading and notch are kept constant whereas the back grading was modified to obtain several GGI profiles with ΔGGI ranging from 0 to approximately 0.8 (See Figure S1). More details and material parameters used can be found elsewhere.[14]

3 | RESULTS AND DISCUSSION

3.1 | Back grading modification

In this study, Ga back gradings were tuned by changing the evaporation rates of In and Ga during the first coevaporation stage, as shown in Figure 1A. Solid lines show the evaporation rates of our reference process, estimated from the sources temperature setpoints. Three different approaches are investigated to modify the back gradings. The corresponding samples are identified with R, G, I and O letters, representing reference, Ga series, In series and early stage In-free series. For comparison, the depth profile of reference R1 is shown in Figure 1(B), (C) and (D) as a reference. The height of the back grading is measured with the quantity ΔGGI, defined as the difference between the minimum GGI value in the notch and its maximum near the back interface. The equivalent E_g energy is calculated by Equation (1).[18]

$$E_g = 1.004(1-\mathrm{GGI}) + 1.663\mathrm{GGI} - 0.033\mathrm{GGI}(1-\mathrm{GGI}) \quad (1)$$

In the first and second approach, we implemented steeper gallium source cooling rates (dashed blue line G in Figure 1A), and steeper indium source heating rates (dashed green line I in Figure 1A) in the first stage. However, the attempts only resulted in moderate changes in the corresponding composition profiles shown in Figure 1B,C.

A third approach was developed to further increase ΔGGI: the indium shutter is kept closed during the initial minutes of the deposition process, while the source temperature settings were the same as those for the baseline process, as illustrated by an orange block (O) in Figure 1A. Therefore, the absorber is In-free during the initial minutes of the deposition process. The corresponding depth profiles are shown in Figure 1D. With this approach, the highest ΔGGI value of 0.5 was obtained, equivalent to about 0.33 eV. In the different deposition runs, Ga and In source temperatures were adjusted by small constant offsets over the whole process, in order to compensate for drifts in the source evaporation yields and achieve similar integrated GGI and optical bandgaps. Table 1 compares the J-V parameters of solar cells with different ΔGGI investigated in this study. Detailed process sequences for each sample can be found in Table S1. Integrated GGI values for those samples range from 0.28 to 0.35 and CGI values are almost within the confidence interval of the composition measurements. Short-circuit current density (J_{SC}) is in good agreement with calculated EQE currents and the fill factor (FF) is similar for all samples. The most sensitive parameter is the V_{OC}, which is analyzed in the following.

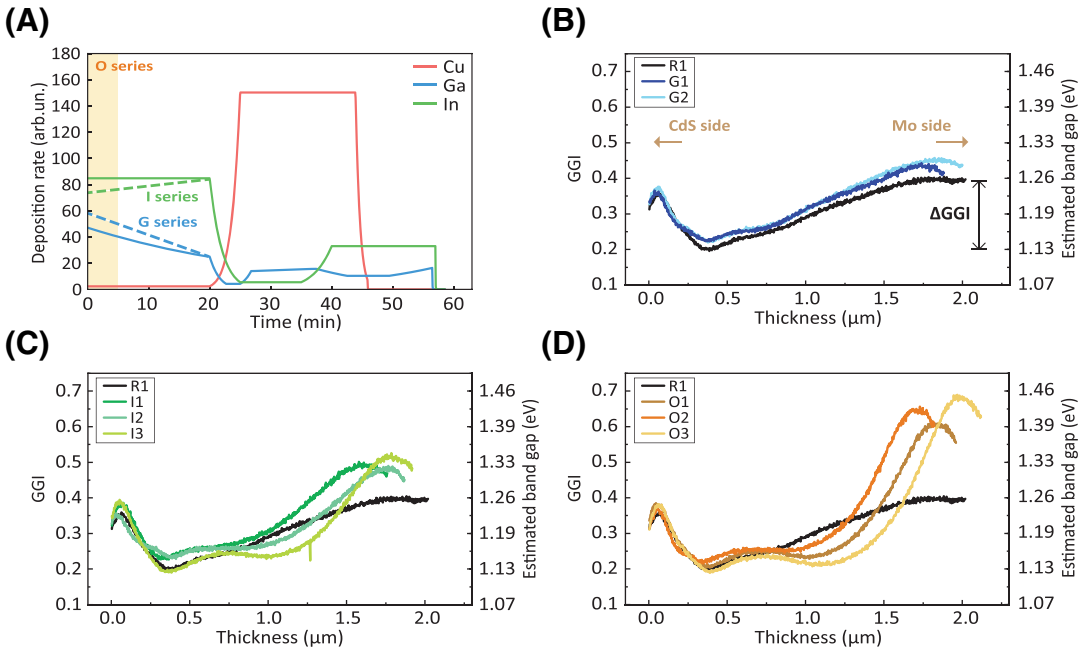

FIGURE 1 (A) Schematic representation of a multi-stage deposition with indicative Cu, In, Ga evaporation rates. The solid lines represent the baseline process. The dashed lines and orange block show three different approaches to modify the back grading. (B) GGI and E_g depth profiles for different Ga source cooling rates. E_g is calculated by Equation (1). (C) GGI and E_g depth profiles for different In source heating rates. (D) GGI and E_g depth profiles for different In-free periods in early stage In-free series [Colour figure can be viewed at wileyonlinelibrary.com]

TABLE 1 Composition of CIGS absorbers with different ΔGGI and the corresponding J-V parameters

					Photovoltaic parameters				
Sample	GGI	CGI	E_g(eV)	ΔGGI	V_{OC} (V)	J_{SC} (mA cm^{-2})	*FF* (%)	PCE (%)	V_{OC} deficit (V)
R1	0.31	0.86	1.144	0.20	0.686	35.3	77.6	18.8	0.458
R2	0.32	0.87	1.142	0.20	0.679	36.3	77.5	19.1	0.463
G1	0.33	0.88	1.138	0.21	0.687	35.2	77.1	18.7	0.451
G2	0.34	0.90	1.140	0.23	0.695	35.6	76.9	19.0	0.445
I1	0.34	0.88	1.147	0.26	0.703	35.0	76.8	19.0	0.444
I2	0.32	0.91	1.137	0.25	0.693	35.6	77.1	19.0	0.444
I3	0.31	0.88	1.123	0.32	0.697	35.8	76.4	19.1	0.429
I4	0.28	0.88	1.121	0.29	0.685	36.7	77.4	19.5	0.436
O1	0.34	0.89	1.132	0.41	0.707	36.0	77.0	19.6	0.425
O2	0.35	0.90	1.150	0.43	0.723	35.2	77.5	19.7	0.427
O3	0.34	0.87	1.135	0.50	0.716	35.4	76.2	19.3	0.419

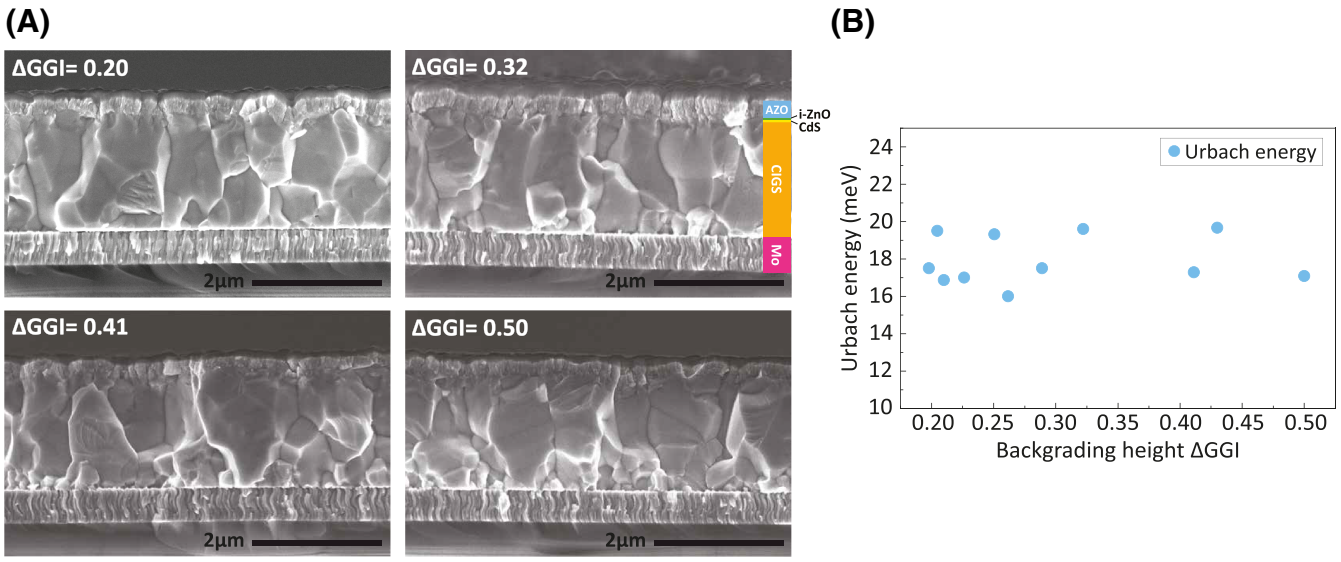

FIGURE 2 (A) SEM cross-section images for solar cells (R1, I3, O1 and O3) with different ΔGGI. An increased Ga content towards the back of the absorber leads to reduced grain size at back region, while the microstructure in the front and notch regions appear unchanged. (B) Urbach energy (E_U) versus different ΔGGI. No clear correlation is evidenced between E_U and ΔGGI [Colour figure can be viewed at wileyonlinelibrary.com]

In addition to the composition profiles, the microstructure in the front and notch was investigated by cross-section SEM to identify possible deterioration of the microstructure. As shown in Figure 2A, the grain size is similar for all the absorbers in the front and notch regions. A decrease in grain size is only observed towards the back, especially for absorbers with high ΔGGI. This observation is consistent with existing reports describing a decrease in grain size with increased Ga content.[19]

Apart from changes in the microstructure, the presence of structural and electronic defects is also investigated through the Urbach tails.[20] The Urbach energy (E_U) is estimated from the quasi-exponential decay in the long wavelength edge in the EQE curves.[2] As shown in Figure 2B, there is no clear trend of E_U with ΔGGI. The precision on the values is not better than ±2 meV due to the presence of interference fringes in the EQE spectra. The values derived from EQE measurements are typically slightly larger than those derived from PL, due to the higher energy range for which the fit is performed.

GGI depth profiles, SEM cross-sectional images and extracted E_U show no noticeable impact on the front and notch regions from increased ΔGGI at least up to 0.5. Therefore, different electrical loss between samples is mostly caused by different back recombination, instead of changed properties either in the front or notch regions.

3.2 | V_{OC} deficit and ΔGGI

To see the effect of ΔGGI on the electrical loss, $V_{OC,def}$ is also given in Table 1, which is calculated from the E_g energy and V_{OC}. The E_g value

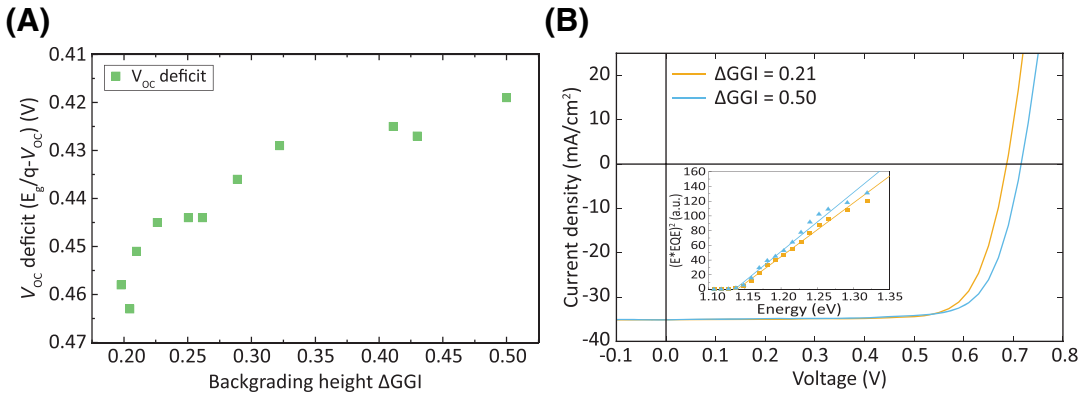

FIGURE 3 (A) $V_{OC,def}$ of the investigated samples as a function of their ΔGGI values. (B) J-V curves and E_g extraction for two selected solar cells with similar E_g but different ΔGGI values [Colour figure can be viewed at wileyonlinelibrary.com]

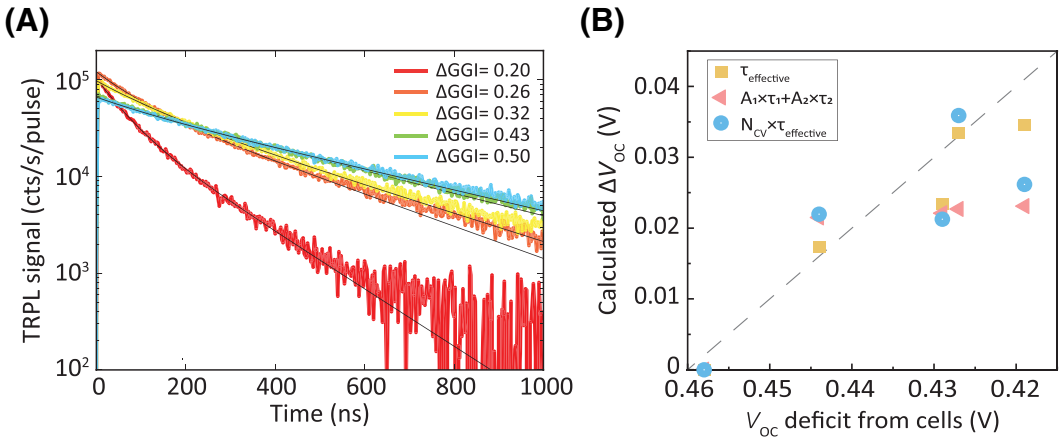

FIGURE 4 (A) TRPL transients of absorbers with different ΔGGI. The black lines are best 2-exponential fits to the data from 20 to 500 ns. (B) ΔV_{OC} calculated from different figures of merit using Equation (5) as function of the experimental cell $V_{OC,def}$ [Colour figure can be viewed at wileyonlinelibrary.com]

was determined by linear extrapolation of the plot ((photon energy × EQE)^2 vs. photon energy) for values between 25% and 75% of the EQE maximum.

Figure 3A shows the change of $V_{OC,def}$ values with different ΔGGI. An evident improvement in $V_{OC,def}$ with higher ΔGGI is observed. The $V_{OC,def}$ values improved by about 35 mV when ΔGGI is increased from 0.20 to 0.32. For ΔGGI increase from 0.32 to 0.50, an additional V_{OC} gain of 10 mV is observed. However, this 10 mV gain can also be explained by sample to sample variation, measurement uncertainty or E_g extraction. To obtain more solid evidence on the improved $V_{OC,def}$ in the full range of ΔGGI, TRPL measurements were conducted and are discussed in following sections.

J-V curves of two solar cells (G1 and O3) with similar E_g but different ΔGGI (0.21 and 0.50) are compared in Figure 3B. The corresponding E_g extractions are shown in the inset. Sample O3 exhibits a strongly increased V_{OC} due to higher ΔGGI. The J_{SC} is comparable for both solar cells, consistent with their similar bandgaps. Due to the improvement in V_{OC}, photovoltaic conversion efficiency (PCE) is increased from 18.7% to 19.3%. PCE of the champion cell in this study is about 19.7%.

3.3 | TRPL lifetime and ΔGGI

$V_{OC,def}$ is a device parameter related to overall electrical loss at the device level whereas TRPL decays provide direct information of carrier dynamics in the absorbers that can be linked to its material quality. Therefore, the relationship between TRPL lifetime and ΔGGI is investigated to see if high ΔGGI values up to at least 0.50 still contributes to reduction in electrical losses, as discussed in Section 3.2.

TRPL measurements were performed on selected absorbers covering different ΔGGI values as shown in Figure 4A. The decays were fitted from 20 ns to 500 ns by a two-exponential formula (Equation 2) with two time constants (τ_1 and τ_2). The effective lifetime τ_{eff} is calculated using Equation (3). As visible in Figure 4A absorbers with high ΔGGI show considerably longer lifetimes as compared with low ΔGGI ones, suggesting a reduction in back interface recombination.

$$Y = A_1 \exp\left(-\frac{t}{\tau_1}\right) + A_2 \exp\left(-\frac{t}{\tau_2}\right) \quad (2)$$

$$\tau_{\text{eff}} = \frac{A_1\tau_1 + A_2\tau_2}{A_1 + A_2} \tag{3}$$

We further calculated the theoretical change in V_{OC} based on TRPL decays. Equation (4) describes the relationship between achievable V_{OC} and external light emitting-diode quantum efficiency (EQE_{LED}).[21] From this, the difference in achievable V_{OC} (ΔV_{OC}) of different samples is evaluated according to Equation (5). Here, we estimated the ratio of EQE_{LED} with the ratio of different figure of merits (FOMs) from the TRPL data. The absorber with a ΔGGI of 0.20 was chosen as the reference providing a ΔV_{OC} of 0 mV.

$$V_{\text{OC,def}}^{\text{non-rad}} = V_{\text{OC}}^{\text{rad}} - V_{\text{OC}} = -\frac{kT}{q}\ln(\text{EQE}_{\text{LED}}) \tag{4}$$

$$\begin{aligned}\Delta V_{\text{OC}} &= V_{\text{OC,def}\ \text{ref}}^{\text{non-rad}} - V_{\text{OC,def}\ \text{sample}}^{\text{non-rad}} \\ &= \frac{kT}{q}\ln\left(\frac{\text{EQE}_{\text{LED,sample}}}{\text{EQE}_{\text{LED,ref}}}\right) \\ &= \frac{kT}{q}\ln\left(\frac{\text{FOM}_{\text{sample}}}{\text{FOM}_{\text{ref}}}\right)\end{aligned} \tag{5}$$

Three different FOMs are established to compare the EQE_{LED} of different samples relatively: (1) τ_{eff}, (2) $A_1 \times \tau_1 + A_2 \times \tau_2$ and (3) $N_{CV} \times \tau_{\text{eff}}$. For τ_{eff}, it was assumed that the doping density is the same for those absorbers. For the second FOM, the prefactors (A_1 and A_2) were taken into account. The sum of prefactor terms are assumed to be proportional to the doping density of the absorbers. For the third FOM, the doping density N_{CV} extracted directly from C-V measurements at V=0 (See Figure S2) is used instead of prefactors from TRPL decays. Figure 4B shows the relationship between calculated ΔV_{OC} from those three FOMs and $V_{\text{OC,def}}$ measured from cells. Among them, τ_{eff} gives a better correlation with $V_{\text{OC,def}}$ from cells. This can be explained by the non-uniform doping density distribution within a sample. While the bandgaps were always extracted from EQE measurement of the best cell in the sample, TRPL and C-V measurements were performed on the cells close to the best cell. To avoid the variations from the doping density, different calculated ΔV_{OC} will be further discussed in Section 3.5.

3.4 | Back surface modification

In addition to back interface recombination, variations in TRPL decays may also arise from different non-radiative recombination rates elsewhere, for example, within the bulk of the absorber. To extract the effect solely from the increasing ΔGGI, we further measured TRPL decays on the same series of samples after different modifications of the back interface. It also helps to understand how far high graded CIGS absorbers are from the ideal case (i.e. no back interface recombination).

After the initial measurement described in Section 3.3, the CIGS absorbers were mechanically delaminated from the molybdenum back contact with a transparent epoxy glue, as depicted in Figure 5A. The exposed CIGS/air interface results in a lower back surface recombination velocity[22] than the CIGS/Mo contact. After TRPL characterization, the back surface was further passivated by 30 nm Al_2O_3 deposited by ALD. The concept of Al_2O_3 passivation was shown to effectively reduce recombination at CIGS/Mo[23] or CIGS/air interfaces.[24] According to the literature,[22-25] those three different back surfaces cover different values of surface recombination velocity, ranging from about 10^7 to 10^2 cm/s.

Figure 5B displays the TRPL results obtained with different sample configurations. We observe an increase in lifetime after delamination, and a further increase after Al_2O_3 deposition. Improvements are especially significant for absorbers with low ΔGGI values, being three-fold for ΔGGI= 0.20 and only 1.25 times for ΔGGI = 0.50 after delamination. This is explained by the reduced electron density at the back with higher ΔGGI, resulting in a lesser sensitivity to the surface recombination velocity value. The three-fold increase for ΔGGI = 0.20 can be attributed to the difference of interface recombination velocity at CIGS/air (on the order of 10^3 cm/s) and CIGS/Mo (>10^6 cm/s). As example, Figure 5C,D shows TRPL decays for samples with low and high ΔGGI. The decays are very similar for high ΔGGI, while being very different for small ΔGGI. It suggests that back surface recombination is a strong limiting factor for V_{OC}, and that its effect can be observed with ΔGGI values up to 0.50. In addition, the τ_{eff} value is still slightly improved with increasing ΔGGI after 30 nm Al_2O_3 deposition. This can be explained by a low but non-negligible recombination at CIGS/air interface,[22] further passivated by Al_2O_3.

3.5 | Numerical simulation

To support the experimental findings of Figure 5, we carried out finite element modelling simulations. Here we are interested in the effect of back recombination solely from varying ΔGGI and its implications on V_{OC}. Different bandgap profiles are implemented into 2 μm-thick absorbers, in which only the back grading has been modified to achieve ΔGGI values ranging from 0 to a maximum of 0.8. For simplicity, back recombination velocity is fixed to $S_b \gg 10^7$ cms^{-1}. Other recombination velocities found at CIGS/Mo interface (e.g. 10^6 cms^{-1} in Weiss et al.[22]) also show similar results in our simulation. Since back recombination is highly sensitive to the diffusion length of carriers, that is, $L_d = \sqrt{\frac{kT}{q}\mu\tau}$, we consider a wide range of carrier mobility μ (12.5 $cm^2V^{-1}s^{-1}$ to 200 $cm^2V^{-1}s^{-1}$) and τ (approximately 100 to 800 ns) covering the range of values typically found experimentally. The ΔV_{OC} of a simulated device is calculated as the V_{OC} difference from that with highest ΔGGI of 0.80.

Experimentally, it is difficult to exclude effects on V_{OC} arising from deviations in absorber doping concentration or bandgap that could occur between different growth runs. Thus, instead of Equation (5), we compute the relative ΔV_{OC} before and after delamination (Equation 6), for absorbers with different ΔGGI. By doing this, possible deviations in the aforementioned material properties (doping or E_g) are discriminated for the same absorber and the effect of ΔGGI can be analyzed.

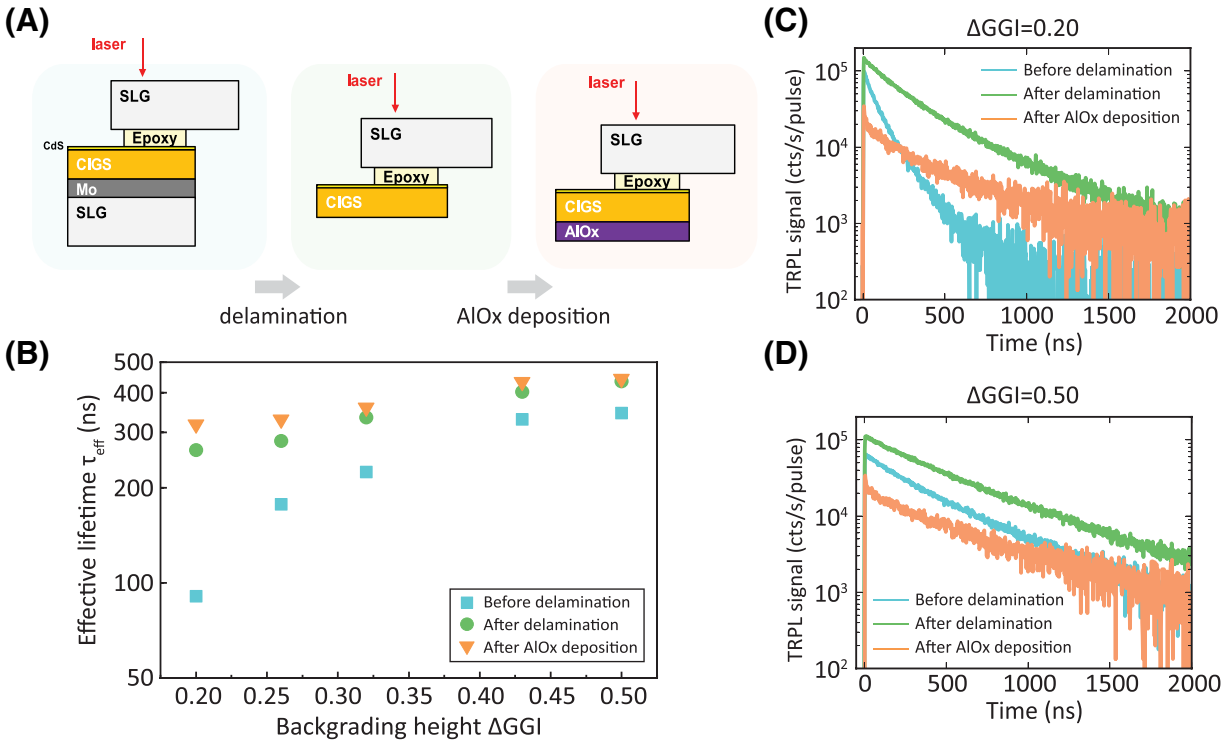

FIGURE 5 (A) Schematics of back surface modification and the corresponding TRPL measurements. (B) TRPL τ_{eff} for absorbers in three different sample configurations. (C) TRPL decays for the absorbers with ΔGGI = 0.20, and (d) ΔGGI = 0.50 [Colour figure can be viewed at wileyonlinelibrary.com]

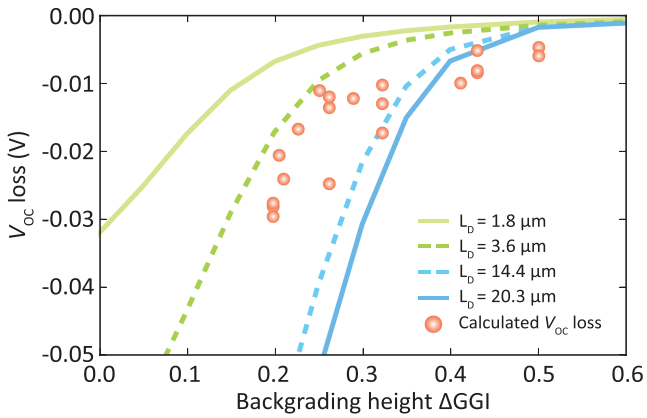

FIGURE 6 Experimental and simulation results for the estimation of V_{OC} loss. Orange circles are the V_{OC} loss calculated from experimental TRPL decays (Equation 6) before and after delamination. For simulated absorbers, two solid curves depict the upper and lower limit of L_d (1.8 to 20.3 μm). Two dashed curves correspond to the range of L_d (3.6 to 14.4 μm) fitting best our experimental results (orange data points) [Colour figure can be viewed at wileyonlinelibrary.com]

Figure 6 shows simulation results for several L_d values as a function of ΔGGI, together with the experimental ΔV_{OC} calculated by Equation (6) (orange circles) of the samples listed in Table 1. Two dashed lines in Figure 6 establish the upper and lower bound for L_d values that could reproduce the experimental results (L_d between 3.6 and 14.4 μm), which are in good agreement with other reports.[13,14,22] The solid lines are shown as extreme instances to exemplify the degree of V_{OC} loss sensitivity with respect to L_d. The V_{OC} loss is strongly dependent on the L_d value but almost insensitive to the actual combination of μ and τ used to obtain the L_d value. From Section 3.4 and Figure 5B, we expect a τ_{eff} around 400 ns in our absorbers. By assuming a τ_{eff} of 400 ns, mobilities in the range of 12.5 to 200 $cm^2V^{-1}s^{-1}$ are suggested, with the best fit corresponding to μ=50 $cm^2V^{-1}s^{-1}$ and L_d approximately 7 μm, which are in good agreement with.[22] Within this range of L_d values, simulations confirm that ΔGGI = 0.3 leads to a significant voltage loss about 7 to 20 mV. The voltage loss becomes insignificant (<5 mV) for ΔGGI around 0.5, independently of the L_d value. Hence, a ΔGGI ≥ 0.5 is needed to ensure a voltage loss below 5 mV, especially with long diffusion length. Finally, we use the simulations to quantify the beneficial impact of the backgrading. We quantify a substantial voltage gain around 91 ± 28 mV between ΔGGI=0 and ΔGGI=0.3, with deviations defined by the two dashed lines of Figure 6. This value is consistent with what is reported in Feurer et al.[26] (114 mV) for a pure $CuInSe_2$ case.

$$V_{OC}\ \text{loss} = -\frac{kT}{q}\ln\left(\frac{\tau_{eff,\,after\,del}}{\tau_{eff,\,before\,del}}\right) \quad (6)$$

4 | CONCLUSION

We have successfully modified the height of the compositional back grading ΔGGI in CIGS absorbers for solar cells applications. The combination of low substrate temperature and early stage In-free coevaporation allows to widely tune the ΔGGI value without significant changes in microstructure and structural disorder in the low

E_g notch and front regions of the absorber, as indicated by SEM and Urbach energy values. This allows a more rigorous comparison between cells with different ΔGGI in this study.

The $V_{OC,def}$ improves up to a ΔGGI value of about 0.50, and TRPL τ_{eff} shows a similar trend with increased ΔGGI. We observe a strong correlation between $V_{OC,def}$ calculated from cells and voltage losses ΔV_{OC} estimated from TRPL τ_{eff}. In addition, absorbers with high ΔGGI show less sensitivity of the TRPL decays to modifications of the back surface properties, i.e. different recombination velocity. We conclude that back surface recombination affects device performance in a measurable manner up to a ΔGGI of 0.50. We also quantify the impact of diffusion length on the voltage loss from the back interface with numerical simulations. Reasonable parameter sets yield V_{OC} loss trends in good agreement with our experimental results. We believe our results will provide useful guidelines for designing GGI profiles for high-quality CIGS absorbers. The proposed In-free process step makes it easier to optimize ΔGGI for existing baseline processes while maintaining almost unchanged composition and properties in the front and notch.

ACKNOWLEDGEMENTS

This work received funding from Swiss Federal Office of Energy (SFOE) under ImproCIS project (Contract no.: SI/501614-01) and from the Swiss State Secretary for Education, Research and Innovation (SERI) under contract number 17.00105 (EMPIR project HyMet). The EMPIR programme is co-financed by the participating States and by the European Union's Horizon 2020 research and innovation programme.

ORCID

Shih-Chi Yang https://orcid.org/0000-0002-0312-4194

REFERENCES

1. Nakamura M, Yamaguchi K, Kimoto Y, Yasaki Y, Kato T, Sugimoto H. Cd-Free Cu(In,Ga)(Se,S) $_2$ thin-film solar cell with record efficiency of 23.35%. *IEEE J Photovoltaics*. 2019;9(6):1863-1867.
2. Carron R, Nishiwaki S, Feurer T, et al. Advanced alkali treatments for high-efficiency Cu(In,Ga)Se2 solar cells on flexible substrates. *Adv Energy Mater*. 2019;9(24):1900408.
3. Scheer R, Schock H-W. *Chalcogenide Photovoltaics: Physics, Technologies, and Thin Film Devices*. Weinheim, Germany: Wiley-VCH Verlag GmbH & Co. KGaA; 2011.
4. Gorji NE, Perez MD, Reggiani U, Sandrolini L. A new approach to valence and conduction band grading in CIGS thin film solar cells. *IJET*. 2012;4(5):573-576.
5. Contreras MA, Tuttle J, Gabor A, et al. High efficiency Cu(In,Ga)Se/sub 2/-based solar cells: Processing of novel absorber structures. In: Proceedings of 1994 IEEE 1st World Conference on Photovoltaic Energy Conversion - WCPEC (A Joint Conference of PVSC, PVSEC and PSEC), Waikoloa, HI, USA. Vol. 1; 1994:68-75 vol.1.
6. Dullweber T, Lundberg O, Malmström J, et al. Back surface band gap gradings in Cu(In,Ga)Se2 solar cells. *Thin Solid Films*. 2001;387(1):11-13.
7. Gloeckler M, Sites JR. Band-gap grading in Cu(In,Ga)Se2 solar cells. *J Phys Chem Solids*. 2005;66(11):1891-1894.
8. Gloeckler M. Device physics of copper(indium,gallium)selenide (2) thin-film solar cells. *Ph.D.*: Colorado State University; 2005.
9. Frisk C, Platzer-Björkman C, Olsson J, et al. Optimizing Ga-profiles for highly efficient Cu(In, Ga)Se $_2$ thin film solar cells in simple and complex defect models. *J Phys D: Appl Phys*. 2014;47(48):485104.
10. Amin N, Chelvanathan P, Hossain MI, Sopian K. Numerical modelling of ultra thin Cu(In,Ga)Se2 solar cells. *Energy Proc*. 2012;15:291-298.
11. Ouedraogo S, Sam R, Ouedraogo F, et al. Optimization of Copper Indium Gallium Di-Selenide (CIGS) based solar cells by back grading. In: *2013 Africon*. Pointe aux Piments, Mauritius; 2013:1-6.
12. Jackson P, Hariskos D, Wuerz R, et al. Properties of Cu(In,Ga)Se2 solar cells with new record efficiencies up to 21.7%. *Phys Stat Solidi (RRL) Rapid Res Lett*. 2015;9(1):28-31.
13. Kato T, Wu J-L, Hirai Y, Sugimoto H, Bermudez V. Record efficiency for thin-film polycrystalline solar cells up to 22.9% achieved by Cs-Treated Cu(In,Ga)(Se,S)2. *IEEE J Photovoltaics*. 2019;9(1):325-330.
14. Ochoa M, Buecheler S, Tiwari AN, Carron R. Challenges and opportunities for an efficiency boost of next generation Cu(In,Ga)Se2 solar cells: Prospects for a paradigm shift. *Energy Environ Sci*. 2020;13(7):2047-2055.
15. Klinkert T, Jubault M, Donsanti F, Lincot D, Guillemoles J-F. Ga gradients in Cu(In,Ga)Se $_2$: Formation, characterization, and consequences. *J Renew Sustain Energy*. 2014;6(1):11403.
16. Avancini E, Carron R, Bissig B, et al. Impact of compositional grading and overall Cu deficiency on the near-infrared response in Cu(In, Ga)Se2 solar cells. *Prog. Photovolt. Res. Appl*. 2017;25(3):233-241.
17. Sentaurus. Sentaurus Device User Guide. p. version P-2019.3; 2019.
18. Carron R, Avancini E, Feurer T, et al. Refractive indices of layers and optical simulations of Cu(In,Ga)Se2 solar cells. *Sci Technol Adv Mater*. 2018;19(1):396-410.
19. Jung S, Ahn S, Yun JH, Gwak J, Kim D, Yoon K. Effects of Ga contents on properties of CIGS thin films and solar cells fabricated by co-evaporation technique. *Current Appl Phys*. 2010;10(4):990-996.
20. Chantana J, Nishimura T, Kawano Y, Teraji S, Watanabe T, Minemoto T. Examination of relationship between urbach energy and open-circuit voltage deficit of flexible Cu(In,Ga)Se2 solar cell for its improved photovoltaic performance. *ACS Appl Energy Mater*. 2019;2(11):7843-7849.
21. Rau U. Reciprocity relation between photovoltaic quantum efficiency and electroluminescent emission of solar cells. *Phys Rev B*. 2007;76(8):85303.
22. Weiss TP, Bissig B, Feurer T, Carron R, Buecheler S, Tiwari AN. Bulk and surface recombination properties in thin film semiconductors with different surface treatments from time-resolved photoluminescence measurements. *Sci Rep*. 2019;9(1):5385.
23. Vermang B, Fjällström V, Pettersson J, Salomé P, Edoff M. Development of rear surface passivated Cu(In,Ga)Se2 thin film solar cells with nano-sized local rear point contacts. *Solar Energy Mater Solar Cells*. 2013;117:505-511.
24. Bissig B. Micro- and macroscopic characterization of recombination losses in high efficiency Cu(In,Ga)Se2 thin film solar cells. *Doctoral Thesis*: ETH Zurich; 2018.
25. Bissig B, Guerra-Nunez C, Carron R, et al. Surface passivation for reliable measurement of bulk electronic properties of heterojunction devices. *Small*. 2016;12(38):5339-5346.
26. Feurer T, Bissig B, Weiss TP, et al. Single-graded CIGS with narrow bandgap for tandem solar cells. *Sci Technol Adv Mater*. 2018;19(1):263-270.

SUPPORTING INFORMATION

Additional supporting information may be found online in the Supporting Information section at the end of this article.

How to cite this article: Yang S-C, Ochoa M, Hertwig R, Aribia A, Tiwari AN, Carron R. Influence of Ga back grading on voltage loss in low-temperature co-evaporated Cu(In,Ga)Se2 thin film solar cells. *Prog Photovolt Res Appl*. 2021;29:630–637. https://doi.org/10.1002/pip.3413